O-GlcNAcase contributes to cognitive function in Drosophila

Muha, Villo; Fenckova, Michaela; Ferenbach, Andrew; Catinozzi, Marica ; Eidhof, Ilse ; Storkebaum, Erik

Published in:
Journal of Biological Chemistry

DOI:
10.1074/jbc.RA119.010312

Publication date:
2020

Document Version
Peer reviewed version

O-GlcNAcase contributes to cognitive function in *Drosophila*

Villő Muha[1+], Michaela Fenckova[1,2+], Andrew T. Ferenbach[1], Marica Catinozzi[3], Ilse Eidhof[2], Erik Storkebaum[3], Annette Schenck[2] and Daan M. F. van Aalten[1]*

From the [1]Gene Regulation and Expression, School of Life Sciences, University of Dundee, Dundee, UK; [2]Department of Human Genetics, Donders Institute for Brain, Cognition and Behaviour, Radboud University Medical Center, 6525GA, Nijmegen, Netherlands; [3]Department of Molecular Neurobiology, Donders Institute for Brain, Cognition and Behaviour and Faculty of Science, Radboud University, Nijmegen, Netherlands

Running title: *Drosophila Oga is required for habituation learning*

[+]These authors contributed equally to this work

*To whom correspondence should be addressed: Daan M. F. van Aalten: Gene Regulation and Expression, School of Life Sciences, University of Dundee, Dundee, UK, Email: dmfvanaalten@dundee.ac.uk

Keywords: O-GlcNAcylation, O-GlcNAcase, learning, habituation, *Drosophila*, NMJ

ABSTRACT

O-GlcNAcylation is an abundant post-translational modification in neurons. In mice, an increase in O-GlcNAcylation leads to defects in hippocampal synaptic plasticity and learning. O-GlcNAcylation is established by two opposing enzymes O-GlcNAc transferase (OGT) and O-GlcNAcase (OGA). To investigate the role of OGA in elementary learning, we generated catalytically inactive and precise knock-out *Oga* alleles (Oga^{D133N} and Oga^{KO}, respectively) in *Drosophila melanogaster.*

Adult Oga^{D133N} and Oga^{KO} flies lacking O-GlcNAcase activity showed locomotor phenotypes. Importantly, both *Oga* lines exhibited deficits in habituation, an evolutionary conserved form of learning, highlighting that the requirement for O-GlcNAcase activity for cognitive function is preserved across species. Loss of O-GlcNAcase affected number of synaptic boutons at the axon terminals of larval neuromuscular junction. Taken together, we report behavioral and neurodevelopmental phenotypes associated with *Oga* alleles and show that Oga contributes to cognition and synaptic morphology in *Drosophila*.

Introduction

Protein O-GlcNAcylation, a dynamic modification of proteins with N-acetylglucosamine on serine/threonine residues, is orchestrated by two enzymes, O-GlcNAc transferase (OGT) and O-GlcNAcase (OGA). O-GlcNAcylation maintains cellular homeostasis by modulating translation (1), protein stability (2, 3) and subcellular localization of proteins (4, 5). Furthermore, it plays a key role in regulating transcription (6–9) and differentiation (10, 11). Although the mechanism of O-GlcNAcylation is highly evolutionary conserved, from the early metazoan *Trichoplax adhaerens* to humans (12), there are considerable differences in the extent vertebrates and invertebrates tolerate alteration in protein O-GlcNAcylation.

OGA, the enzyme which removes the O-GlcNAc modification, is the product of the *MGEA5* (meningioma-expressed antigen 5) gene in vertebrates. OGA is indispensable for late embryonic development and postnatal survival of mammals (13, 14). Mouse pups lacking OGA protein show delayed development, small size, abnormality in lung histology and perinatal lethality (13, 14). *Drosophila Oga null* mutants, however, develop normally to adulthood (15, 16), making *Drosophila* an attractive system for uncovering previously unappreciated roles of OGA.

A substantial body of evidence indicates that O-GlcNAcylation is crucial for normal development and function of the mammalian nervous system (17–21). In mice, increased O-GlcNAcylation induced by a brain-specific knockout of OGA manifested in a delay in brain development, reduced olfactory bulb size, missing anterior pituitary, enlarged brain

ventricles, and revealed that OGA is required for neurogenesis (22). It has recently been established that certain mutations in the human OGT gene cause intellectual disability (23–26). The mutations are associated with reduced OGA mRNA and protein levels (23, 27, 28) suggesting that altered OGA expression may contribute to the diverse developmental and cognitive symptoms in these patients. Furthermore, recently identified SNPs in the intronic sequence of *OGA* have associated the gene with IQ and intellectual development (29), together indicating a role for OGA in human cognition.

Recent studies have demonstrated that both acute and chronic increases of protein O-GlcNAcylation cause hippocampus-associated learning and memory defects in mice and rats (30, 31). Despite these studies suggesting a crucial function of OGA in normal learning, our knowledge about how OGA affects cognitive ability is limited. Therefore, we investigated if the role of OGA in learning is conserved in *Drosophila*.

OGA is a multi-domain protein; it consists of an N-terminal O-GlcNAc hydrolase catalytic domain that belongs to the GH84 family of glycoside hydrolases (32), a middle highly disordered 'stalk' domain and a C-terminus with sequence homology to histone acetyltransferases (HATs). The HAT domain lacks key amino acids responsible for acetyl-coenzyme A binding (33), thus OGA only exhibits O-GlcNAcase enzymatic activity. However, it has never been investigated before if OGA possesses any non-enzymatic roles. Therefore, we also developed tools to dissect enzymatic or non-enzymatic functions of Oga in normal neuronal development and cognition/learning.

We generated rationally designed catalytically inactive *Oga* (Oga^{D133N}) and a novel *Oga* knockout (Oga^{KO}) alleles by exploiting the CRISPR/Cas9 gene editing toolbox, resulting in elevated levels of protein-O-GlcNAcylation in homozygous flies. We discovered that a loss of O-GlcNAcase activity affects locomotion and causes deficits in habituation learning, thereby demonstrating a conserved role of *Drosophila Oga* in cognitive function. Additionally, we showed that synaptic bouton counts at the larval neuromuscular junctions are altered in Oga^{KO} flies indicating a novel role for *Oga* in synaptic development. Our phenotypic characterisation of Oga^{D133N} and Oga^{KO} lines also revealed that the primary role of *Oga* in these processes is O-GlcNAcase enzyme activity.

Results

Genome editing of Oga results in increased protein O-GlcNAcylation

In order to dissect O-GlcNAcase enzymatic and any non-enzymatic roles of OGA, we generated catalytically inactive and precise null *Drosophila Oga* alleles (**Fig. 1A**). The *Drosophila* Oga protein shows 57 % sequence identity with the human enzyme (hOGA). Previous studies have identified a conserved aspartate, D175 in hOGA as a key catalytic amino acid in both vertebrate and bacterial OGAs (34–36). This residue is D133 in *Drosophila* Oga, and, together with the rest of the catalytic machinery, conserved throughout evolution (**Supplementary Fig. S1).** Mutation of this aspartate to an asparagine leads to a protein species incapable of hydrolysis, yet with retention of O-GlcNAc protein binding (37–39). We have used a CRISPR/Cas9 gene editing approach to introduce the D133N mutation into the endogenous *Oga,* thus generating the desired catalytically inactive (Oga^{D133N}) allele. Parallelly, we isolated a null allele (Oga^{KO}) produced by 2 nucleotides frameshift mutation at 3R:21219675 [+] (Oga mRNA 547 nucleotide position) resulting in a premature STOP codon and a truncated 148 amino acid long peptide product (**Supplementary Fig. S2)**.

Homozygous Oga^{D133N} and Oga^{KO} animals developed to adulthood without apparent defects. To probe the effect of the newly generated *Oga* alleles on O-GlcNAc homeostasis, samples from Oga^{D133N} and Oga^{KO} embryos and adult heads were subjected to Western blotting (**Fig. 1B and 1C**). Oga was undetectable in homozygous Oga^{KO} samples **(Fig. 1B and 1C)**, while it was expressed at wild type level in heterozygous Oga^{D133N} ($Oga^{D133N/+}$) and homozygous Oga^{D133N} flies (**Fig. 1C**). Half gene dosage of *Oga* in $Oga^{KO/+}$ flies led to approximately 60% reduction in protein level (normalized expression: $w^{1118} = 1$, $Oga^{KO/+} = 0.40 \pm 0.1$) (**Fig. 1D**). Protein O-GlcNAcylation levels were 2.2-fold elevated in samples from both homozygous Oga^{D133N} and Oga^{KO} flies (**Fig. 1E**). In summary, we created two new alleles of *Oga* that showed increased protein O-GlcNAcylation and enabled the dissection of Oga function.

Compromised Oga function leads to a reduction in lifespan and locomotor defects in adult flies

Elevated O-GlcNAc levels due to high sugar and high glucosamine diet are known to shorten median lifespan of adult flies (40). We first tested whether the increased protein O-GlcNAcylation in *Oga* mutant flies affects survival as a measure of overall health. Batches of 20 male flies collected within 24 hours past eclosion were placed into vials with standard diet and their lifespan was monitored for over 100 days. The mean lifespan for genetic background control flies was 73.0 ± 1.4 days, while homozygous Oga^{D133N} (61.1 ± 0.8 days) and Oga^{KO} (67.2 ± 0.7 days) adult males exhibited significant mean lifespan reduction of approximately twelve and six days, respectively (**Fig. 2A)**.

Loss of OGT in mouse post-mitotic neurons caused a rapid increase of daily food intake accompanied with hyperactivity (21), indicating that the O-GlcNAc system potentially influences locomotor activity of an organism. Therefore, we tested daily locomotor activity in Oga^{D133N} and Oga^{KO} male adults using DAM2 *Drosophila* activity monitors. Under 12:12 h of light: dark cycle condition, the Oga^{KO} group consistently showed a modest, but significant decrease in total daily activity counts (mean ± SD, 1088 ± 266 total activity counts/day) compared to control (1359 ± 371) and Oga^{D133N} (1350 ± 345) groups (**Fig. 2B, Supplementary Fig. S3A-S3C**). Furthermore, the Oga^{KO} flies exhibited a reduction in activity counts while awake (**Supplementary Fig. S3D-S3F)** suggesting that the observed lower daily activity is possibly associated with motor defects.

Hence, we next further explored motor phenotypes in Oga^{D133N} and Oga^{KO} flies using island test and negative geotaxis assays. Both tests are widely used to investigate neuronal impairment and muscular defects in *Drosophila* models of intellectual disability, neurodegeneration and neuromuscular diseases (41–44). The island test measures escape responses requiring activation and coordination of leg and wing movements. In this assay, flies are thrown onto a white flat platform surrounded with water, and the time each individual spends on the platform is determined. Healthy wild type flies normally exhibit an escape response and quickly fly away from the platform. Under the island assay test conditions, homozygous Oga^{D133N} (3700 ± 1300) and Oga^{KO} (area under curve parameter (AUC), mean ± SD; 5200 ± 1100) flies remained markedly longer on the platform than the background control line (1900 ± 1000) (**Fig. 2C and 2D**).

In the negative geotaxis assay, young (2-4 days old) male control flies climbed at a mean speed of 23 ± 5 mm/s. However, climbing performance of homozygous Oga^{D133N} (17 ± 7 mm/s) and Oga^{KO} (18 ± 6 mm/s) flies showed significantly reduced climbing speed compared to genetic background controls, indicating locomotor impairment (**Fig. 2E**).

Taken together, these data show that compromised *Oga* function leads to reduced lifespan and locomotor defects in adult flies.

Loss of Drosophila Oga and its O-GlcNAcase activity causes deficits in habituation learning

To dissect possible role of Oga in cognition, we investigated the effect of *Oga* mutations on habituation. Habituation is a fundamental, evolutionary conserved form of learning characterized by a temporal attenuation of an initial strong response to a repeated, irrelevant stimulus. It is an important prerequisite for higher cognitive functioning and has been found to be defective in a number of neurodevelopmental disorders in humans (45, 46) and animal models (47–49). To assess the role of Oga and its O-GlcNAcase catalytic activity in this type of learning we subjected Oga^{D133N} and Oga^{KO} flies and isogenic genetic background control flies to 100 short (15 ms) light-off stimuli with 1 s intervals in the light-off jump habituation assay. Locomotor deficits observed in the negative geotaxis and island assay did not preclude assessment of habituation, as assessed by a fatigue assay (**Supplementary Fig. S4).** All fly lines were able to exhibit good initial jump responses to the first five light-off stimuli (>50% initial jumpers, **Supplementary Table S2)**. Control flies habituated quickly to the repeated light-off stimulus (mean ± SEM TTC = 4.3 ± 0.5, n = 65, **Fig. 3A** and 7.2 ± 0.8, n = 74, **3B**). Both homozygous *Oga* mutant lines showed slow habituation and failed to adapt their jump response to the repeated stimulus (Oga^{D133N}: 53.8 ± 3.7, mean TTC fold-change = 7.5, n = 86; Oga^{KO}: mean ± SEM TTC = 10.1 ± 2.3, mean TTC fold-change compared to control flies = 2.3, n = 63; **Fig. 3A-3D, Supplementary Table S2**). We generated and tested also pan-neuronal

Oga knockdown flies (*elav>Oga*^{RNAi}), using an inducible *Oga* UAS-RNAi allele (VDRC *#41822),* and the pan-neuronal elav-Gal4 driver, to address the neuronal/glial-specificity of these defects**.** Progeny from crosses between the *elav-Gal4* driver line and the genetic background of the RNAi line *(VDRC #60000*) were used as controls. The knockdown flies showed good initial jump response (70.8 % initial jumpers) but failed to habituate compared to controls (mean ± SEM TTC = 12.9 ± 2.5, mean TTC fold-change = 4.2, n = 68, **Fig. 3E and 3F, Supplementary Table S2**). Taken together, these data show that loss of *Drosophila* Oga and its O-GlcNAcase activity leads to a deficit in habituation learning and that Oga activity in neurons is required for habituation.

O-GlcNAcase modulates the number of synaptic boutons at the larval neuro-muscular junction

Normal synaptic development and morphology are crucial for motor behaviour, learning and cognitive functioning. Importantly, a significant number of proteins that orchestrate synapse structure and synaptic transmission are modified with O-GlcNAc (50, 51), including in *Drosophila* (38). We next investigated synaptic morphology in *Oga*^{D133N} and *Oga*^{KO} flies. The larval neuro-muscular junction (NMJ) is a well-established system to study synaptic development and morphology in *Drosophila*. Type 1b NMJs consist of branched chains of synaptic boutons containing glutamatergic transmission sites, which share fundamental mechanistic features with the excitatory system in the mammalian brain (52). We visualized the larval NMJ architecture by immunolabeling the presynaptic marker synaptotagmin (Syt) and postsynaptic Discs large 1 (Dlg1) proteins (**Fig. 4A**). Morphometric features of individual muscle 4 NMJs were quantified semi-automatically (53)(54). We detected mean values of area, perimeter and length in *Oga*^{D133N} and *Oga*^{KO} NMJs similar to those in controls (**Supplementary Fig. S5**). The numbers of synaptic islands, branches and branching points were also unaffected in the *Oga* mutants (**Supplementary Fig. S5**). However, we observed a modest increase in the number of boutons in *Oga*^{D133N} NMJs, which did not reach statistical significance (mean ± SD; 34.4 ± 7.6), and a significant increase in *Oga*^{KO} (36.5 ± 7.9) compared to background control (30.7 ± 7.3) larval NMJs (**Fig. 4B**). These data indicate that Oga potentially influences the number of synaptic boutons at the axon terminals at the larval neuromuscular junction.

Discussion

Earlier studies have uncovered a link between O-GlcNAcase and learning in mouse and rat models (30, 31). Heterozygous *Oga*$^{+/-}$ mice with increased O-GlcNAc levels exhibited hippocampal-dependent spatial learning and memory defects (31), while rats treated with an OGA inhibitor, thiamet-G, showed reduced performance in novel object and placement tests (30). These learning phenotypes were associated with dysregulation of synaptic plasticity, long-term synaptic potentiation (LTP) and AMPA Receptor (AMPAR)-dependent long-term synaptic depression (LTD) (30). Several O-GlcNAc-modified proteins were found that operate at the mammalian synapse, such as Bassoon, Piccolo and Synapsin (51), regulate transcriptional programs relevant to synaptic plasticity in neurons, such as the cyclic-AMP-response element binding protein (CREB) (55), control neuronal microtubule dynamics such as tau (56) and CRMP2 (57), or mediate synaptic transmission, such as AMPAR Glu2 subunit (30). O-GlcNAcylation on these and other proteins together potentially modulates neuronal functions. Although the molecular mechanism behind these learning and synaptic phenotypes are not fully understood, our current knowledge indicates that synergic response of multiple voltage-gated ion channels (58) and dysregulation of AMPAR are involved (31, 58).

In contrast to mammalian organisms where MGEA5/OGA is crucial for embryonic development (13, 14), *Oga* is not essential in *Drosophila melanogaster* (15, 16) and *Caenorhabditis elegans* (59). However, the fact that the *Oga* gene is conserved across invertebrates suggests that maintenance of homeostatic O-GlcNAc levels by OGA may provide a considerable advantage to Metazoa. Previous work has shown that knock down of *Oga* in the fly leads to altered metabolism through effects on insulin producing cells (60, 61). Some of the phenotypes, for example the life span effects that we observe here (**Fig. 2A**) could be a manifestation of this. However, we also demonstrated that *Oga*^{KO} and *Oga*^{D133N} mutations lead to deficits in habituation, highlighting that the role of OGA in learning is

evolutionary conserved. Our data also provide evidence that the *Drosophila* nervous system is sensitive to an increase of the level of O-GlcNAcylation and absence of OGA, establishing it as a suitable genetic model system to study underlying mechanisms and substrates involved.

It has been reported previously that increased protein O-GlcNAcylation caused impaired synaptic plasticity in $Oga^{+/-}$ mice without affecting dendritic spine density in CA1 pyramidal neurons (31). Here, we report that bouton number of the larval NMJ is affected in Oga^{KO} null mutants, showing that synaptic morphology is altered in Oga^{KO} animals.

Although Oga^{D133N} and Oga^{KO} caused changes in protein O-GlcNAcylation to the same extent, we described behavioural and neuronal phenotypes that manifested to a different degree in the two *Oga* lines. Reduction of total daily activity and an increase in NMJ bouton number was only apparent in Oga^{KO}, while this genotype appeared to exhibit less severe habituation deficits. A possible explanation of this lies in the choice of inactivating mutation. Previous work in mammalian and bacterial O-GlcNAcases has shown that the equivalent of the D133N mutation inactivates the enzyme. However, recent work has uncovered that this mutation does not lose the ability to bind O-GlcNAc proteins – indeed this inactive mutant can be used to enrich the O-GlcNAc proteome (38, 62**).** Therefore, it is possible that the D133N mutation contributes to the stronger habituation phenotype by binding to (parts of) the O-GlcNAc proteome in the fly, interfering with O-GlcNAc signaling/sites. Thus the Oga^{D133N} potentially behaves as a neomorphic allele. It is possible that absence or presence of the Oga protein affects the phenotypes. For example, the reduction in daily activity and an increase in NMJ bouton number specific for the Oga^{KO} allele might emerge as a combined effect of lack of Oga activity and absence of the Oga protein. Our results thus suggest that such additional functions could modulate the phenotypes arising from complete loss of O-GlcNAcase activity.

In summary, we have shown that *Oga* regulates O-GlcNAc homeostasis thus influencing lifespan, locomotor and neuronal performance in *Drosophila melanogaster*. Further studies are required to define the mechanisms downstream of *Oga* that affect neuronal development or function, resulting in synaptic morphology and habituation learning defects.

Experimental procedures

Cloning of the guide RNA and repair template DNA vectors for Drosophila CRISPR/Cas9 editing

Drosophila melanogaster lines lacking Oga activity, Oga^{KO} and Oga^{D133N}, were generated using the CRISPR/Cas9 gene editing technique following a workflow as previously described (Mariappa et al., 2018). A guide RNA site was selected with the help of the crispr.mit.edu online tool search and the annealing primer pair (gRNA_oga_fwd and gRNA_oga_rev) with appropriate overhangs for *Bpi*I restriction digestion were cloned into pCFD3-dU63gRNA plasmid (63). A vector coding for repair template DNA of 2044 base pairs was generated from *Drosophila* Schneider 2 cell genomic DNA by PCR using GoTaq G2 Polymerase (Promega), A1fix_BAM_fwd, A1fix_NOT_rev primers. The PCR product was inserted into pGEX6P1 plasmid. The desired mutation, in addition to five silent mutations (**Supplementary Fig. S2**) was introduced by site directed mutagenesis using the paired primers D133N wobble F and R. The silent mutations removed a neighbouring $Taq^{\alpha}I$ restriction site, thus enabling genotyping based on restriction digestion. DNA products of cloning and mutagenesis were confirmed by sequencing. All primer sequences are listed in **Supplementary Table S2.**

Generation of Oga^{D133N} and Oga^{KO} Drosophila lines

Drosophila embryos expressing Cas9 in the germline cells (vasa::Cas9, Bloomington stock #51323) were injected with a cocktail of CRISPR/Cas9 reagents, 100 ng/µl guideRNA plasmid and 300 ng/µl repair template DNA vector. Microinjections were performed at the University of Cambridge fly facility. Founder male flies were crossed with *Dr/Tm6* balancer stock in-house. Subsequently, single potential Oga^{D133N}*/Tm6* germline mutant male flies and *Dr/Tm6* virgins were crossed that allowed for elimination of the *vasa::Cas9* carrying X chromosome. Candidate F1 males were genotyped exploiting restriction fragment length polymorphism arising from the loss of $TaqI^{\alpha}$ restriction digestion site introduced in parallel with the D133N mutation **(Supplementary Fig. S2A)**. We recovered a knock-in line carrying the

precise mutation, Oga^{D133N}; and a knock-out line where a frame shift resulting from non-homologous end joining repair of a CRISPR event introduced a premature STOP codon into the *Oga* sequence, Oga^{KO} **(Supplementary Fig. S2B)**. Lines were validated first by sequencing the diagnostic digest PCR product confirming the region approximately 250 base pairs upstream and downstream of the mutation. This was followed by production of larger PCR products encompassing an area outside the repair template. Sequencing of these products confirmed that only the intended changes were introduced to *Oga* and excluded the possibility of ectopic integration of the repair template somewhere else in the genome. In order to eliminate any potential off-target mutations introduced during CRISPR, our *Oga* lines were backcrossed into the w^{1118} control genetic background for six generations prior to experimentation.

Restriction fragment length polymorphism assay for genotyping Oga^{D133N} and Oga^{KO} *lines*

To assess and confirm presence of the D133N and KO mutation in *Oga* gene, candidate individual adult flies were frozen and homogenized in 10-50 µl of DNA extraction buffer containing 10 mM Tris-HCl pH 8, 1 mM EDTA, 25 mM NaCl and 200 µg/ml freshly added Proteinase K (Roche) and subsequently incubated at 37 °C for 30 min, followed by inactivation of Proteinase K at 95 °C for 3 min, and centrifuged briefly. 1 µl of the crude DNA extract was used per 25 µl PCR reaction with A1_DIG F and R primers and KOD Hot start polymerase (Novagen). 5 µl of the 589 bp PCR product was used for restriction fragment length polymorphism assay with $Taq^{\alpha}I$ followed by agarose gel electrophoresis of the digested products. Full length fragments resistant to $Taq^{\alpha}I$ cleavage indicated CRISPR/Cas9 gene editing event and were sequenced using A1_DIG primers. Precise incorporation of the repair template into the right position of the genome was confirmed by sequencing a second round of PCR products obtained from potential homozygous CRISPR mutants with mixed A1_DIG and A1_OOB primer pairs. Primer sequences are listed in **Supplementary Table S2.**

Fly stocks and maintenance

All *Drosophila* strains and crosses were reared on a standard *Drosophila* diet (sugar/cornmeal/yeast). Unless stated otherwise all crosses were raised at 25 °C, 70% humidity and 12:12 h light-dark cycle.

RNAi strain against *Drosophila Oga* (*#41822*, zero predicted off-targets, >60 % reported knockdown efficiency (60) and a control strain (*#60000*) were obtained from Vienna Drosophila Resource Center (VDRC; www.vdrc.at).

Oga^{D133N} and Oga^{KO} strains were crossed into the VDRC w^{1118} control genetic background for six generations. This isogenic background strain was used as control for experiments on Oga^{D133N} and Oga^{KO} strains. The w^{1118}*; 2xGMR-wIR; elav-Gal4, UAS-Dicer-2* driver strain was used to induce neuronal knockdown. This strain contains a double insertion of an RNAi construct targeting the gene *white* specifically in the *Drosophila* eye (*2xGMR-wIR*) to suppress pigmentation, as required for an efficient jump response in light-off jump habituation (49, 64, 65). Progeny of the cross between the RNAi strain and the respective genetic background was tested in habituation experiments.

Western blotting from Drosophila samples

To prepare protein lysates for Western blotting, homozygous parental flies were set up in egg laying cups with apple juice plates at 25 °C. 4-8h embryos were collected, dechorionated with bleach and snap frozen in liquid nitrogen. Also, 1-4 days old adult male flies were collected and snap frozen in liquid nitrogen. Heterozygous flies were obtained from crossing Oga^{KO} and Oga^{D133N} with w^{1118}. Heads were separated by vigorous vortexing for 2 x 15 sec. The frozen samples were homogenized in 2 µl / 1 head lysis buffer containing 2x NuPAGE LDS Sample Buffer, 50 mM Tris- HCl (pH 8.0), 150 mM NaCl, 4 mM sodium pyrophosphate, 1 mM EDTA, 1 mM benzamidine, 0.2 mM PMSF, 5 µM leupeptin and 1% 2-mercaptoethanol. Lysates were then heated for 5 min at 95 ºC, centrifuged at 13000 rpm for 10 min and supernatants were collected. Protein concentrations were estimated using the Pierce 660 nm protein assay supplemented with Ionic Detergent Compatibility Reagent (Thermo Scientific). Protein concentrations were adjusted across samples. 20 - 30 µg of protein lysate was loaded on NuPAGE 4-12% Bis-Tris protein gels (Invitrogen) and transferred onto nitrocellulose membrane. Membranes were developed with mouse anti-O-GlcNAc antibody, RL2 (1:1000, Thermo), rabbit anti-OGT (1:1000, Abcam, ab-96718), rabbit anti-OGA (1:1000, Sigma,

SAB4200267) and rabbit anti-actin (1:5000, Sigma, A2066) primary antibodies and donkey anti mouse IgG 800 and goat anti-rabbit IgG 680 infrared dye conjugated secondary antibodies (Li-Cor, 1: 10000). Western blots were recorded on a Licor system and signal was measured using Lite software. Significance was calculated using one-way ANOVA with Dunnett's multiple comparisons test.

Measurement of lifespan

20 age-matched male flies were placed in a vial within 24 h of eclosion for recording their lifespan. Flies were flipped in every 2-3 days and number of flies alive were recorded. At least 9 vials (Control 9, Oga^{KO} 14 and Oga^{D133N} 14 vials) for each genotype were tracked. Vials were kept in the same tray and incubator at 25°C and 12:12 h light-dark cycle. Log-rank test was used to compare lifespan across genotypes.

Drosophila activity monitoring

Drosophila locomotor activity was monitored using the DAM2 Drosophila Activity Monitoring System (TriKinetics) at 25°C and 12:12 h light-dark cycle, using 2-3 days old male flies. The method was described in detail previously (66). Food mixture containing 2 % agar, 5 % sucrose was loaded to one end of 65 mm tubes. Activity was recorded for 5 days, data obtained on the 2nd to 5th days were used and merged for this study. Datasets were analysed using the Sleep and Circadian Analysis MATLAB Program (S.C.A.M.P.) (67). Combined data from four independent measurements with 20-30 flies per genotype was analysed, statistical significance was calculated using one-way ANOVA with Bonferroni's multiple comparisons test.

Island assay

The island assay was used to evaluate the flight locomotor behaviour of the 2-3 days-old male flies as described previously (68, 69). 15 flies from every genotype were subjected to the assay per run. 3-4 repeats were carried out on each day, and data was collected on 3 consecutive days, in total we collected data from 9-12 runs per genotype. Area under curve (AUC) was determined for each run, groups were compared using ANOVA with Holm-Sidak's multiple comparisons of means for AUC.

Negative geotaxis test

Climbing assay was performed as described previously (43). Briefly, 0-2 days old male flies were collected and divided into groups of 10 animals at least 48 h before the measurement. Climbing ability of 3-6 days old flies was evaluated. On the day of the measurement, flies were transferred into 150 x 16 mm transparent plastic test tubes without anaesthesia. Maximum ten test tubes were placed into a frame that allowed for monitoring of climbing behaviour of up to 100 animals at once. The frame was secured onto an apparatus that releases the frame from a fixed height upon pushing a button. The frame falls down onto a mouse pad, thereby tapping the flies to the bottom of the tubes. The climbing assay was repeated 4 times for each loaded frame providing data from 4 runs. The whole procedure was recorded with a Nikon D3100 DSLR camera. The resulting movies were then analysed with ImageJ/FIJI software. First, the images were converted to 8-bit grey scale TIFF image sequence (10 frames per second) file format. Following background-subtraction and filtering, the image sequences were binarized to allow for tracking of flies using the MTrack3 plug-in. Mean climbing speed (mm / s) was quantified for each genotype in each run, between 19-89 data points were collected per run. Groups were compared using Mann-Whitney test on mean climbing speed values calculated for each run.

Light-off jump habituation

The light-off jump reflex habituation assay was performed as previously described (49, 70). Briefly, 32 individual 3- to 7-day-old male flies were transferred in the habituation chambers of two independent 16-unit light-off jump habituation systems. Male progeny of the control genetic background was tested simultaneously and served as control in all experiments. Flies were tested at 25°C and 70% humidity. They were exposed to a series of 100 light-off stimuli (stimulus duration was 15 ms) with 1 s interstimulus interval. The noise amplitude of wing vibration accompanying the jump response was recorded after the start of each stimulus. An automatic threshold was applied to distinguish the jump responses from background noise. Data were collected by a custom-made Labview Software (National Instruments). High initial jump responses to light-off stimulus decreased with the repetition of the stimuli and flies were deemed habituated when they failed to jump in five consecutive trials (no-jump criterion). Habituation was

quantified as the number of trials required to reach the no-jump criterion (Trials To Criterion (TTC)). All experiments were done in triplicates (N=96 flies). Despite reduced locomotion abilities of Oga^{KO} and Oga^{D133N} observed in island and climbing assay, these mutant genotypes exhibited sufficient initial jump responses to the light-off stimuli to allow habituation to be assessed (>50% initial jumpers, **Supplementary Table S2**). Main effects of genotype on log-transformed TTC values were tested using a linear model regression analysis (lm) in the R statistical software (R version 3.0.0 (2013-04-03) (71) and corrected for the effects of testing day and habituation system.

Fatigue assay

The assay measures the ability of flies to perform the jumping task repeatedly for prolonged time. This test was carried out subsequently after the habitation assay on the same flies with each genotype as described previously (49). Jump response is induced with a light-off pulse, however the interval time between light-off pulses was adjusted to 5 seconds, a long enough period to prevent the formation of habitation response. The light-off stimuli were repeated 50 times. Jump response of mutant groups were compared to the appropriate control genotype. Flies, that maintained similar jump response to control groups over the 50 trails, were interpreted as fit for the habituation assay.

Analysis of synaptic morphology

Crosses for all mutants and controls were set up with 1-3 days old 5 female virgin and 10 male flies. The adults were flipped out after 36 hours from the vials. This step prevented larval crowding, ensured proper staging and equal size of the larvae. The size of the larvae was also examined by the experimenter prior to dissection. Wandering male L3 larvae were dissected with an open book preparation (72) and fixed in 3.7% paraformaldehyde for 30 minutes. Larvae were stained overnight at 4°C with the primary antibodies against the following synaptic markers: Discs large (anti-dlg1, mouse, 1:25, Developmental Studies Hybridoma Bank), synaptotagmin (anti-Syt, rabbit, 1:2000, kindly provided by H. Bellen). Then the samples were stained with secondary antibodies (1:500) anti-mouse Alexa 488 and anti-rabbit Alexa 568 (Invitrogen) for 2 h at room temperature. Projections of type 1b neuromuscular junctions (NMJs) at muscle 4 from abdominal segments A2-A4 were visualized with Zeiss Axio Imager Z2 microscope with Apotome. Individual synapses were imaged and quantified using an in-house developed macro (53, 54) in Fiji (version 1.49 (73). NMJ area, length, number of branches and branching points were analyzed based on discs large labeling and the number of synaptic boutons was analyzed based on synaptotagmin labeling. Parameters with normal distribution (area, length, number of boutons) were compared between the mutants and control with one-way ANOVA with Tukey's multiple comparison test. Parameters without normal distribution (number of branches and branching points) were compared with non-parametric Wilcoxon test. Statistical analysis was carried out in SPSS.

Acknowledgements
We thank Mehmet Gundogdu, Vasudha Vandadi and Daniel Mariappa for their invaluable help and comments. This work was in part funded by a TOP grant (912-12-109) from The Netherlands Organisation for Scientific Research (NWO) to AS and by a Wellcome Trust Senior Research Fellowship (WT087590MA) to D.M.F.v.A. This work also received funding from the Donders Center for Neuroscience (to ES) and the Muscular Dystrophy Association (MDA, to ES).

Author contributions
V.M., M.F. and D.M.F.v.A. conceived the study; V.M, M.F., A.T.F., and M.C. performed experiments; V.M. and M.F. analysed data; I.E. and M.C. assisted with experiments and data analysis and V.M., M.F., E.S., A.S. and D.M.F.v.A. interpreted the data and wrote the manuscript with input from all authors.

Conflict of interest
No conflict of interests.

References

1. Zhu, Y., Liu, T.-W., Cecioni, S., Eskandari, R., Zandberg, W. F., and Vocadlo, D. J. (2015) O-GlcNAc occurs cotranslationally to stabilize nascent polypeptide chains. *Nat. Chem. Biol.* **11**, 319–325
2. Chu, C.-S., Lo, P.-W., Yeh, Y.-H., Hsu, P.-H., Peng, S.-H., Teng, Y.-C., Kang, M.-L., Wong, C.-H., and Juan, L.-J. (2014) O-GlcNAcylation regulates EZH2 protein stability and function. *Proc. Natl. Acad. Sci. U. S. A.* **111**, 1355–60
3. Gambetta, M. C., and Müller, J. (2014) O-GlcNAcylation Prevents Aggregation of the Polycomb Group Repressor Polyhomeotic. *Dev. Cell*. **31**, 629–639
4. Skorobogatko, Y., Landicho, A., Chalkley, R. J., Kossenkov, A. V., Gallo, G., and Vosseller, K. (2014) *O* -Linked β- *N* -Acetylglucosamine (*O* -GlcNAc) Site Thr-87 Regulates Synapsin I Localization to Synapses and Size of the Reserve Pool of Synaptic Vesicles. *J. Biol. Chem.* **289**, 3602–3612
5. Peng, C., Zhu, Y., Zhang, W., Liao, Q., Chen, Y., Zhao, X., Guo, Q., Shen, P., Zhen, B., Qian, X., Yang, D., Zhang, J.-S., Xiao, D., Qin, W., and Pei, H. (2017) Regulation of the Hippo-YAP Pathway by Glucose Sensor O-GlcNAcylation. *Mol. Cell*. **68**, 591-604.e5
6. Constable, S., Lim, J.-M., Vaidyanathan, K., and Wells, L. (2017) O-GlcNAc transferase regulates transcriptional activity of human Oct4. *Glycobiology*. **27**, 927–937
7. Lamarre-Vincent, N., and Hsieh-Wilson, L. C. (2003) Dynamic glycosylation of the transcription factor CREB: a potential role in gene regulation. *J. Am. Chem. Soc.* **125**, 6612–3
8. Ranuncolo, S. M., Ghosh, S., Hanover, J. A., Hart, G. W., and Lewis, B. A. (2012) Evidence of the involvement of O-GlcNAc-modified human RNA polymerase II CTD in transcription in vitro and in vivo. *J. Biol. Chem.* **287**, 23549–61
9. Deplus, R., Delatte, B., Schwinn, M. K., Defrance, M., Méndez, J., Murphy, N., Dawson, M. A., Volkmar, M., Putmans, P., Calonne, E., Shih, A. H., Levine, R. L., Bernard, O., Mercher, T., Solary, E., Urh, M., Daniels, D. L., and Fuks, F. (2013) TET2 and TET3 regulate GlcNAcylation and H3K4 methylation through OGT and SET1/COMPASS. *EMBO J.* **32**, 645–55
10. Andres, L. M., Blong, I. W., Evans, A. C., Rumachik, N. G., Yamaguchi, T., Pham, N. D., Thompson, P., Kohler, J. J., and Bertozzi, C. R. (2017) Chemical Modulation of Protein O-GlcNAcylation *via* OGT Inhibition Promotes Human Neural Cell Differentiation. *ACS Chem. Biol.* **12**, 2030–2039
11. Jang, H., Kim, T. W., Yoon, S., Choi, S.-Y., Kang, T.-W., Kim, S.-Y., Kwon, Y.-W., Cho, E.-J., and Youn, H.-D. (2012) O-GlcNAc regulates pluripotency and reprogramming by directly acting on core components of the pluripotency network. *Cell Stem Cell*. **11**, 62–74
12. Hart, G. W., Housley, M. P., and Slawson, C. (2007) Cycling of O-linked β-N-acetylglucosamine on nucleocytoplasmic proteins. *Nature*. **446**, 1017–1022
13. Yang, Y. R., Song, M., Lee, H., Jeon, Y., Choi, E.-J., Jang, H.-J., Moon, H. Y., Byun, H.-Y., Kim, E.-K., Kim, D. H., Lee, M. N., Koh, A., Ghim, J., Choi, J. H., Lee-Kwon, W., Kim, K. T., Ryu, S. H., and Suh, P.-G. (2012) O-GlcNAcase is essential for embryonic development and maintenance of genomic stability. *Aging Cell*. **11**, 439–48
14. Keembiyehetty, C., Love, D. C., Harwood, K. R., Gavrilova, O., Comly, M. E., and Hanover, J. A. (2015) Conditional knock-out reveals a requirement for O-linked N-Acetylglucosaminase (O-GlcNAcase) in metabolic homeostasis. *J. Biol. Chem.* **290**, 7097–113
15. Radermacher, P. T., Myachina, F., Bosshardt, F., Pandey, R., Mariappa, D., Müller, H.-A. J., and Lehner, C. F. (2014) O-GlcNAc reports ambient temperature and confers heat resistance on ectotherm development. *Proc. Natl. Acad. Sci. U. S. A.* **111**, 5592–7
16. Akan, I., Love, D. C., Harwood, K. R., Bond, M. R., and Hanover, J. A. (2016) Drosophila O-GlcNAcase Deletion Globally Perturbs Chromatin O-GlcNAcylation. *J. Biol. Chem.* **291**, 9906–19
17. Francisco, H., Kollins, K., Varghis, N., Vocadlo, D., Vosseller, K., and Gallo, G. (2009) O-GLcNAc post-translational modifications regulate the entry of neurons into an axon branching program. *Dev. Neurobiol.* **69**, 162–73
18. Lagerlöf, O., Hart, G. W., and Huganir, R. L. (2017) O-GlcNAc transferase regulates

excitatory synapse maturity. *Proc. Natl. Acad. Sci.* **114**, 1684–1689
19. O'Donnell, N., Zachara, N. E., Hart, G. W., and Marth, J. D. (2004) Ogt-Dependent X-Chromosome-Linked Protein Glycosylation Is a Requisite Modification in Somatic Cell Function and Embryo Viability. *Mol. Cell. Biol.* **24**, 1680–1690
20. Wang, A. C., Jensen, E. H., Rexach, J. E., Vinters, H. V, and Hsieh-Wilson, L. C. (2016) Loss of O-GlcNAc glycosylation in forebrain excitatory neurons induces neurodegeneration. *Proc. Natl. Acad. Sci. U. S. A.* **113**, 15120–15125
21. Lagerlöf, O., Slocomb, J. E., Hong, I., Aponte, Y., Blackshaw, S., Hart, G. W., and Huganir, R. L. (2016) The nutrient sensor OGT in PVN neurons regulates feeding. *Science*. **351**, 1293–6
22. Olivier-Van Stichelen, S., Wang, P., Comly, M., Love, D. C., and Hanover, J. A. (2017) Nutrient-driven O-linked N-acetylglucosamine (O-GlcNAc) cycling impacts neurodevelopmental timing and metabolism. *J. Biol. Chem.* **292**, 6076–6085
23. Willems, A. P., Gundogdu, M., Kempers, M. J. E., Giltay, J. C., Pfundt, R., Elferink, M., Loza, B. F., Fuijkschot, J., Ferenbach, A. T., van Gassen, K. L. I., van Aalten, D. M. F., and Lefeber, D. J. (2017) Mutations in N-acetylglucosamine (O-GlcNAc) transferase in patients with X-linked intellectual disability. *J. Biol. Chem.* **292**, 12621–12631
24. Vaidyanathan, K., Niranjan, T., Selvan, N., Teo, C. F., May, M., Patel, S., Weatherly, B., Skinner, C., Opitz, J., Carey, J., Viskochil, D., Gecz, J., Shaw, M., Peng, Y., Alexov, E., Wang, T., Schwartz, C., and Wells, L. (2017) Identification and characterization of a missense mutation in the O-linked β-N-acetylglucosamine (O-GlcNAc) transferase gene that segregates with X-linked intellectual disability. *J. Biol. Chem.* **292**, 8948–8963
25. Bouazzi, H., Lesca, G., Trujillo, C., Alwasiyah, M. K., and Munnich, A. (2015) Nonsyndromic X-linked intellectual deficiency in three brothers with a novel MED12 missense mutation [c.5922G>T (p.Glu1974His)]. *Clin. case reports*. **3**, 604–9
26. Selvan, N., George, S., Serajee, F. J., Shaw, M., Hobson, L., Kalscheuer, V., Prasad, N., Levy, S. E., Taylor, J., Aftimos, S., Schwartz, C. E., Huq, A. M., Gecz, J., and Wells, L. (2018) O-GlcNAc transferase missense mutations linked to X-linked intellectual disability deregulate genes involved in cell fate determination and signaling. *J. Biol. Chem.* **293**, 10810–10824
27. Pravata, V. M., Gundogdu, M., Bartual, S. G., Ferenbach, A. T., Stavridis, M., Õunap, K., Pajusalu, S., Žordania, R., Wojcik, M. H., and van Aalten, D. M. F. (2019) A missense mutation in the catalytic domain of *O* -GlcNAc transferase links perturbations in protein *O* -GlcNAcylation to X-linked intellectual disability. *FEBS Lett.* 10.1002/1873-3468.13640
28. Pravata, V. M., Muha, V., Gundogdu, M., Ferenbach, A. T., Kakade, P. S., Vandadi, V., Wilmes, A. C., Borodkin, V. S., Joss, S., Stavridis, M. P., and van Aalten, D. M. F. (2019) Catalytic deficiency of O-GlcNAc transferase leads to X-linked intellectual disability. *Proc. Natl. Acad. Sci.* **116**, 14961–14970
29. Savage, J. E., Jansen, P. R., Stringer, S., Watanabe, K., Bryois, J., de Leeuw, C. A., Nagel, M., Awasthi, S., Barr, P. B., Coleman, J. R. I., Grasby, K. L., Hammerschlag, A. R., Kaminski, J. A., Karlsson, R., Krapohl, E., Lam, M., Nygaard, M., Reynolds, C. A., Trampush, J. W., Young, H., Zabaneh, D., Hägg, S., Hansell, N. K., Karlsson, I. K., Linnarsson, S., Montgomery, G. W., Muñoz-Manchado, A. B., Quinlan, E. B., Schumann, G., Skene, N. G., Webb, B. T., White, T., Arking, D. E., Avramopoulos, D., Bilder, R. M., Bitsios, P., Burdick, K. E., Cannon, T. D., Chiba-Falek, O., Christoforou, A., Cirulli, E. T., Congdon, E., Corvin, A., Davies, G., Deary, I. J., DeRosse, P., Dickinson, D., Djurovic, S., Donohoe, G., Conley, E. D., Eriksson, J. G., Espeseth, T., Freimer, N. A., Giakoumaki, S., Giegling, I., Gill, M., Glahn, D. C., Hariri, A. R., Hatzimanolis, A., Keller, M. C., Knowles, E., Koltai, D., Konte, B., Lahti, J., Le Hellard, S., Lencz, T., Liewald, D. C., London, E., Lundervold, A. J., Malhotra, A. K., Melle, I., Morris, D., Need, A. C., Ollier, W., Palotie, A., Payton, A., Pendleton, N., Poldrack, R. A., Räikkönen, K., Reinvang, I., Roussos, P., Rujescu, D., Sabb, F. W., Scult, M. A., Smeland, O. B., Smyrnis, N., Starr, J. M., Steen, V. M., Stefanis, N. C., Straub, R. E., Sundet, K., Tiemeier, H., Voineskos, A. N., Weinberger, D. R., Widen, E., Yu, J., Abecasis, G., Andreassen, O. A., Breen, G., Christiansen, L., Debrabant, B., Dick, D. M., Heinz, A., Hjerling-Leffler, J., Ikram, M. A., Kendler, K. S., Martin, N. G., Medland, S. E., Pedersen, N. L., Plomin, R., Polderman, T. J. C., Ripke, S., van der Sluis, S., Sullivan, P. F., Vrieze, S. I., Wright, M. J., and Posthuma, D. (2018) Genome-wide association meta-analysis in 269,867

individuals identifies new genetic and functional links to intelligence. *Nat. Genet.* **50**, 912–919
30. Taylor, E. W., Wang, K., Nelson, A. R., Bredemann, T. M., Fraser, K. B., Clinton, S. M., Puckett, R., Marchase, R. B., Chatham, J. C., and McMahon, L. L. (2014) O-GlcNAcylation of AMPA receptor GluA2 is associated with a novel form of long-term depression at hippocampal synapses. *J. Neurosci.* **34**, 10–21
31. Yang, Y. R., Song, S., Hwang, H., Jung, J. H., Kim, S.-J., Yoon, S., Hur, J.-H., Park, J.-I., Lee, C., Nam, D., Seo, Y.-K., Kim, J.-H., Rhim, H., and Suh, P.-G. (2017) Memory and synaptic plasticity are impaired by dysregulated hippocampal O-GlcNAcylation. *Sci. Rep.* **7**, 44921
32. Cantarel, B. L., Coutinho, P. M., Rancurel, C., Bernard, T., Lombard, V., and Henrissat, B. (2009) The Carbohydrate-Active EnZymes database (CAZy): an expert resource for Glycogenomics. *Nucleic Acids Res.* **37**, D233-8
33. Rao, F. V, Schüttelkopf, A. W., Dorfmueller, H. C., Ferenbach, A. T., Navratilova, I., and van Aalten, D. M. F. (2013) Structure of a bacterial putative acetyltransferase defines the fold of the human O-GlcNAcase C-terminal domain. *Open Biol.* **3**, 130021
34. Dennis, R. J., Taylor, E. J., Macauley, M. S., Stubbs, K. A., Turkenburg, J. P., Hart, S. J., Black, G. N., Vocadlo, D. J., and Davies, G. J. (2006) Structure and mechanism of a bacterial β-glucosaminidase having O-GlcNAcase activity. *Nat. Struct. Mol. Biol.* **13**, 365–371
35. Rao, F. V, Dorfmueller, H. C., Villa, F., Allwood, M., Eggleston, I. M., and van Aalten, D. M. F. (2006) Structural insights into the mechanism and inhibition of eukaryotic O-GlcNAc hydrolysis. *EMBO J.* **25**, 1569–78
36. Cetinbaş, N., Macauley, M. S., Stubbs, K. A., Drapala, R., and Vocadlo, D. J. (2006) Identification of Asp174 and Asp175 as the key catalytic residues of human O-GlcNAcase by functional analysis of site-directed mutants. *Biochemistry*. **45**, 3835–44
37. Schimpl, M., Schüttelkopf, A. W., Borodkin, V. S., and van Aalten, D. M. F. (2010) Human OGA binds substrates in a conserved peptide recognition groove. *Biochem. J.* **432**, 1–7
38. Selvan, N., Williamson, R., Mariappa, D., Campbell, D. G., Gourlay, R., Ferenbach, A. T., Aristotelous, T., Hopkins-Navratilova, I., Trost, M., and van Aalten, D. M. F. (2017) A mutant O-GlcNAcase enriches Drosophila developmental regulators. *Nat. Chem. Biol.* **13**, 882–887
39. Mariappa, D., Selvan, N., Borodkin, V., Alonso, J., Ferenbach, A. T., Shepherd, C., Navratilova, I. H., and vanAalten, D. M. F. (2015) A mutant O-GlcNAcase as a probe to reveal global dynamics of protein O-GlcNAcylation during Drosophila embryonic development. *Biochem. J.* **470**, 255–262
40. Na, J., Musselman, L. P., Pendse, J., Baranski, T. J., Bodmer, R., Ocorr, K., and Cagan, R. (2013) A Drosophila Model of High Sugar Diet-Induced Cardiomyopathy. *PLoS Genet.* **9**, e1003175
41. Kochinke, K., Zweier, C., Nijhof, B., Fenckova, M., Cizek, P., Honti, F., Keerthikumar, S., Oortveld, M. A. W., Kleefstra, T., Kramer, J. M., Webber, C., Huynen, M. A., and Schenck, A. (2016) Systematic Phenomics Analysis Deconvolutes Genes Mutated in Intellectual Disability into Biologically Coherent Modules. *Am. J. Hum. Genet.* **98**, 149–64
42. Eidhof, I., Baets, J., Kamsteeg, E.-J., Deconinck, T., van Ninhuijs, L., Martin, J.-J., Schüle, R., Züchner, S., De Jonghe, P., Schenck, A., and van de Warrenburg, B. P. (2018) GDAP2 mutations implicate susceptibility to cellular stress in a new form of cerebellar ataxia. *Brain*. **141**, 2592–2604
43. Niehues, S., Bussmann, J., Steffes, G., Erdmann, I., Köhrer, C., Sun, L., Wagner, M., Schäfer, K., Wang, G., Koerdt, S. N., Stum, M., Jaiswal, S., RajBhandary, U. L., Thomas, U., Aberle, H., Burgess, R. W., Yang, X.-L., Dieterich, D., and Storkebaum, E. (2015) Impaired protein translation in Drosophila models for Charcot–Marie–Tooth neuropathy caused by mutant tRNA synthetases. *Nat. Commun.* **6**, 7520
44. Mallik, M., Catinozzi, M., Hug, C. B., Zhang, L., Wagner, M., Bussmann, J., Bittern, J., Mersmann, S., Klämbt, C., Drexler, H. C. A., Huynen, M. A., Vaquerizas, J. M., and Storkebaum, E. (2018) Xrp1 genetically interacts with the ALS-associated FUS orthologue caz and mediates its toxicity. *J. Cell Biol.* **217**, 3947–3964
45. McDiarmid, T. A., Bernardos, A. C., and Rankin, C. H. (2017) Habituation is altered in neuropsychiatric disorders-A comprehensive review with recommendations for experimental design and analysis. *Neurosci. Biobehav. Rev.* **80**, 286–305

46. Rigoulot, S., Knoth, I. S., Lafontaine, M.-P., Vannasing, P., Major, P., Jacquemont, S., Michaud, J. L., Jerbi, K., and Lippé, S. (2017) Altered visual repetition suppression in Fragile X Syndrome: New evidence from ERPs and oscillatory activity. *Int. J. Dev. Neurosci.* **59**, 52–59
47. Restivo, L., Ferrari, F., Passino, E., Sgobio, C., Bock, J., Oostra, B. A., Bagni, C., and Ammassari-Teule, M. (2005) Enriched environment promotes behavioral and morphological recovery in a mouse model for the fragile X syndrome. *Proc. Natl. Acad. Sci. U. S. A.* **102**, 11557–62
48. Wolman, M. A., de Groh, E. D., McBride, S. M., Jongens, T. A., Granato, M., and Epstein, J. A. (2014) Modulation of cAMP and ras signaling pathways improves distinct behavioral deficits in a zebrafish model of neurofibromatosis type 1. *Cell Rep.* **8**, 1265–70
49. Fenckova, M., Blok, L. E. R., Asztalos, L., Goodman, D. P., Cizek, P., Singgih, E. L., Glennon, J. C., IntHout, J., Zweier, C., Eichler, E. E., von Reyn, C. R., Bernier, R. A., Asztalos, Z., and Schenck, A. (2019) Habituation Learning Is a Widely Affected Mechanism in Drosophila Models of Intellectual Disability and Autism Spectrum Disorders. *Biol. Psychiatry*. **86**, 294–305
50. Trinidad, J. C., Barkan, D. T., Gulledge, B. F., Thalhammer, A., Sali, A., Schoepfer, R., and Burlingame, A. L. (2012) Global identification and characterization of both O-GlcNAcylation and phosphorylation at the murine synapse. *Mol. Cell. Proteomics*. **11**, 215–29
51. Vosseller, K., Trinidad, J. C., Chalkley, R. J., Specht, C. G., Thalhammer, A., Lynn, A. J., Snedecor, J. O., Guan, S., Medzihradszky, K. F., Maltby, D. A., Schoepfer, R., and Burlingame, A. L. (2006) O-linked N-acetylglucosamine proteomics of postsynaptic density preparations using lectin weak affinity chromatography and mass spectrometry. *Mol. Cell. Proteomics*. **5**, 923–34
52. Menon, K. P., Carrillo, R. A., and Zinn, K. (2013) Development and plasticity of the *Drosophila* larval neuromuscular junction. *Wiley Interdiscip. Rev. Dev. Biol.* **2**, 647–670
53. Nijhof, B., Castells-Nobau, A., Wolf, L., Scheffer-de Gooyert, J. M., Monedero, I., Torroja, L., Coromina, L., van der Laak, J. A. W. M., and Schenck, A. (2016) A New Fiji-Based Algorithm That Systematically Quantifies Nine Synaptic Parameters Provides Insights into Drosophila NMJ Morphometry. *PLoS Comput. Biol.* **12**, e1004823
54. Castells-Nobau, A., Nijhof, B., Eidhof, I., Wolf, L., Scheffer-de Gooyert, J. M., Monedero, I., Torroja, L., van der Laak, J. A. W. M., and Schenck, A. (2017) Two Algorithms for High-throughput and Multi-parametric Quantification of Drosophila Neuromuscular Junction Morphology. *J. Vis. Exp.* 10.3791/55395
55. Rexach, J. E., Clark, P. M., Mason, D. E., Neve, R. L., Peters, E. C., and Hsieh-Wilson, L. C. (2012) Dynamic O-GlcNAc modification regulates CREB-mediated gene expression and memory formation. *Nat. Chem. Biol.* **8**, 253–61
56. Arnold, C. S., Johnson, G. V, Cole, R. N., Dong, D. L., Lee, M., and Hart, G. W. (1996) The microtubule-associated protein tau is extensively modified with O-linked N-acetylglucosamine. *J. Biol. Chem.* **271**, 28741–4
57. Cole, R. N., and Hart, G. W. (2001) Cytosolic O-glycosylation is abundant in nerve terminals. *J. Neurochem.* **79**, 1080–9
58. Hwang, H., and Rhim, H. (2019) Acutely elevated O-GlcNAcylation suppresses hippocampal activity by modulating both intrinsic and synaptic excitability factors. *Sci. Rep.* **9**, 7287
59. Forsythe, M. E., Love, D. C., Lazarus, B. D., Kim, E. J., Prinz, W. A., Ashwell, G., Krause, M. W., and Hanover, J. A. (2006) Caenorhabditis elegans ortholog of a diabetes susceptibility locus: oga-1 (O-GlcNAcase) knockout impacts O-GlcNAc cycling, metabolism, and dauer. *Proc. Natl. Acad. Sci. U. S. A.* **103**, 11952–7
60. Sekine, O., Love, D. C., Rubenstein, D. S., and Hanover, J. A. (2010) Blocking O-linked GlcNAc cycling in Drosophila insulin-producing cells perturbs glucose-insulin homeostasis. *J. Biol. Chem.* **285**, 38684–91
61. Park, S., Park, S.-H., Baek, J. Y., Jy, Y. J., Kim, K. S., Roth, J., Cho, J. W., and Choe, K.-M. (2011) Protein O-GlcNAcylation regulates Drosophila growth through the insulin signaling pathway. *Cell. Mol. Life Sci.* **68**, 3377–3384
62. Schimpl, M., Borodkin, V. S., Gray, L. J., and van Aalten, D. M. F. (2012) Synergy of Peptide

and Sugar in O-GlcNAcase Substrate Recognition. *Chem. Biol.* **19**, 173–178
63. Port, F., Chen, H.-M., Lee, T., and Bullock, S. L. (2014) Optimized CRISPR/Cas tools for efficient germline and somatic genome engineering in Drosophila. *Proc. Natl. Acad. Sci.* **111**, E2967–E2976
64. Willemsen, M. H., Nijhof, B., Fenckova, M., Nillesen, W. M., Bongers, E. M. H. F., Castells-Nobau, A., Asztalos, L., Viragh, E., van Bon, B. W. M., Tezel, E., Veltman, J. A., Brunner, H. G., de Vries, B. B. A., de Ligt, J., Yntema, H. G., van Bokhoven, H., Isidor, B., Le Caignec, C., Lorino, E., Asztalos, Z., Koolen, D. A., Vissers, L. E. L. M., Schenck, A., and Kleefstra, T. (2013) GATAD2B loss-of-function mutations cause a recognisable syndrome with intellectual disability and are associated with learning deficits and synaptic undergrowth in Drosophila. *J. Med. Genet.* **50**, 507–14
65. van Bon, B. W. M., Oortveld, M. A. W., Nijtmans, L. G., Fenckova, M., Nijhof, B., Besseling, J., Vos, M., Kramer, J. M., de Leeuw, N., Castells-Nobau, A., Asztalos, L., Viragh, E., Ruiter, M., Hofmann, F., Eshuis, L., Collavin, L., Huynen, M. A., Asztalos, Z., Verstreken, P., Rodenburg, R. J., Smeitink, J. A., de Vries, B. B. A., and Schenck, A. (2013) CEP89 is required for mitochondrial metabolism and neuronal function in man and fly. *Hum. Mol. Genet.* **22**, 3138–51
66. Chiu, J. C., Low, K. H., Pike, D. H., Yildirim, E., and Edery, I. (2010) Assaying locomotor activity to study circadian rhythms and sleep parameters in Drosophila. *J. Vis. Exp.* 10.3791/2157
67. Donelson, N. C., Donelson, N., Kim, E. Z., Slawson, J. B., Vecsey, C. G., Huber, R., and Griffith, L. C. (2012) High-resolution positional tracking for long-term analysis of Drosophila sleep and locomotion using the "tracker" program. *PLoS One*. **7**, e37250
68. Schmidt, I., Thomas, S., Kain, P., Risse, B., Naffin, E., and Klämbt, C. (2012) Kinesin heavy chain function in Drosophila glial cells controls neuronal activity. *J. Neurosci.* **32**, 7466–76
69. Eidhof, I., Fenckova, M., Elurbe, D. M., van de Warrenburg, B., Castells Nobau, A., and Schenck, A. (2017) High-throughput Analysis of Locomotor Behavior in the Drosophila Island Assay. *J. Vis. Exp.* 10.3791/55892
70. Kramer, J. M., Kochinke, K., Oortveld, M. A. W., Marks, H., Kramer, D., de Jong, E. K., Asztalos, Z., Westwood, J. T., Stunnenberg, H. G., Sokolowski, M. B., Keleman, K., Zhou, H., van Bokhoven, H., and Schenck, A. (2011) Epigenetic regulation of learning and memory by Drosophila EHMT/G9a. *PLoS Biol.* **9**, e1000569
71. Team, R. C. (2008) R: A language and environment for statistical computing
72. Brent, J. R., Werner, K. M., and McCabe, B. D. (2009) Drosophila Larval NMJ Dissection. *J. Vis. Exp.* 10.3791/1107
73. Schindelin, J., Arganda-Carreras, I., Frise, E., Kaynig, V., Longair, M., Pietzsch, T., Preibisch, S., Rueden, C., Saalfeld, S., Schmid, B., Tinevez, J.-Y., White, D. J., Hartenstein, V., Eliceiri, K., Tomancak, P., and Cardona, A. (2012) Fiji: an open-source platform for biological-image analysis. *Nat. Methods*. **9**, 676–82

FOOTNOTES

This work was in part funded by a TOP grant (912-12-109) from The Netherlands Organisation for Scientific Research (NWO) to AS and by a Wellcome Trust Senior Research Fellowship (WT087590MA) to D.M.F.v.A. This work also received funding from the Donders Center for Neuroscience (to ES), the Muscular Dystrophy Association (MDA, to ES), the EU Joint Programme – Neurodegenerative Disease Research (JPND; grant numbers ZonMW 733051075 (TransNeuro) and ZonMW 733051073 (LocalNMD) to ES) and an ERC consolidator grant (ERC-2017-COG 770244 to ES).

Figure Legends

Figure 1. Generation and characterisation of *Oga*^{D133N} and *Oga*^{KO} alleles. (A) Schematic representation of *Drosophila melanogaster* Oga protein; purple glycosyl hydrolase (GH) domain, grey linker domain, green pseudo-histone acetyltransferase domain. The *Oga*^{D133N} allele expresses the full-length *Drosophila* Oga with a single D133N missense mutation in the GH domain (the mutation site is in orange). The *Oga*^{KO} allele only produces a short, truncated polypeptide of 148 amino acids terminating before the catalytic core of Oga GH domain. (B) Western blot on 4-8 h old *Drosophila* embryo samples indicate lack of Oga expression in *Oga*^{KO} line and increased level of O-GlcNAcylation in homozygous *Oga*^{KO} and *Oga*^{D133N} *Drosophila* embryos. Embryos were collected from crosses of homozygous *Oga*^{KO} or *Oga*^{D133N} parental flies. Western blot was probed with an anti-OGA antibody and a monoclonal anti-O-GlcNAc antibody (RL2), raised against O-GlcNAc modified nucleoporins, that recognizes a subset of the O-GlcNAc modified proteome. Actin was used as a loading control. Complete loss of the lower band corresponding to Oga protein was apparent in homozygous (*Oga*^{KO}) samples. (C) Western blot on 1-4 days old male adult head lysates was probed with an anti-OGA antibody and monoclonal anti-O-GlcNAc antibody (RL2). Actin was used as a loading control. The anti-OGA antibody recognizes two proteins at the molecular weight range of 130-180 kDa, the lower band is specific to *Drosophila* Oga and the upper band is non-specific. Complete loss of the lower band was apparent in homozygous *Oga*^{KO} samples. (D) Quantification of Oga protein levels in adult head samples revealed that heterozygous *Oga*$^{KO/+}$ flies have reduced Oga protein compared to genetic background control (one-way ANOVA with Dunnett's multiple comparisons test, $p = 0.036$, n = 3). Oga protein levels are unchanged in heterozygous *Oga*$^{D133N/+}$ and homozygous *Oga*^{D133N} samples ($p = 0.9914$ and $p = 0.9013$, respectively). mean ± SD is shown. (E) Quantification of O-GlcNAcylated proteins revealed that *Oga*^{KO} and *Oga*^{D133N} flies have increased O-GlcNAc levels compared to genetic background control (2.2-fold, one-way ANOVA with Dunnett's multiple comparisons test, $p < 0.0001$, n = 3 for both lines, mean ± SD is shown) *Drosophila* adult head samples.

Figure 2. Lifespan and locomotor behaviour of *Oga*^{KO} and *Oga*^{D133N} flies. (A) Lifespan of homozygous *Oga*^{KO} and *Oga*^{D133N} male flies. Survival of 20 flies per vial was followed until no flies were left alive. Survivorship curves show mean ± SEM of data recorded from 9-14 vials/genotype, scoring the number of flies alive in every 2 days. Log-rank tests indicate decreased mean lifespan for *Oga*^{KO} (n = 280) and *Oga*^{D133N} (n = 280) flies compared to their genetic background control (n = 179) (Control vs *Oga*^{KO}, c2 = 41.5, $p < 0.001$) (Control vs *Oga*^{D133N}, c2 = 104.8, $p < 0.001$). (B) Total daily activity counts of control, *Oga*^{KO} and *Oga*^{D133N} male *Drosophila* plotted in 12:12 h light:dark cycle. *Oga*^{KO} (n = 101) exhibited decreased daily activity compared to control flies (n = 97) ($p < 0.001$, one-way ANOVA with Bonferroni's multiple comparisons test). (C) Locomotion and flight performance were assessed in the island assay. 15 flies per measurement were thrown on a white platform surrounded with water. Graphs show per cent of flies that remain on the platform over time (10 s). Mean ± SEM, for control n = 23, *Oga*^{KO} n = 13, *Oga*^{D133N} n = 14 repeats, data was collected over 3 days of measurement. (D) Floating bars depicting mean ± SD area under curve (AUC) based on the graphs shown in (D), one-way ANOVA with Holm-Sidak's multiple comparisons of mean AUC. Flight escape performance of *Oga*^{KO} and *Oga*^{D133N} flies was impaired compared to control (*Oga*^{KO} $p <$ 0.0001; *Oga*^{D133N} $p = 0.0004$) (E) Climbing locomotor behaviour of Oga deficient flies was assessed based on their climbing speed (mm/s) in an automated negative geotaxis assay. *Oga*^{KO} and *Oga*^{D133N} groups showed significantly reduced climbing speed compared to background control indicating locomotor dysfunction. mean ± SD (Nonparametric Mann-Whitney test, Control n = 14, *Oga*^{D133N} n = 15, $p < 0.0001$; Control n = 15, *Oga*^{KO} n = 15, $p = 0.0002$).

Figure 3. Loss of Oga activity in *Drosophila* affects non-associative learning in the light-off jump reflex habituation paradigm. Jump responses of 3–7-day-old individual male flies were induced by repeated light-off pulses (100 trials) with a 1 s inter-trial interval. Habituation was scored as the mean number of trials required to reach the no-jump criterion (TTC). Jump response curves show the average jump response (% of jumping flies) over 100 light-off trials at 1 s inter-trial interval. The number of trials needed to reach the no-jump criterion is presented as Mean TTC ± SEM. (A) and (B) Habituation of homozygous Oga^{KO} male flies (n = 63) was significantly slower compared to control flies (n = 65) $p = 0.030$. (C) and (D) Habituation of homozygous Oga^{D133N} male flies (n = 86) was significantly slower compared to control flies (n = 74) $p < 0.001$. (E) and (F) Habituation of adult flies with neuronal knockdown of Oga, (elav::GAL4/+; UAS-$Oga^{RNAi41822}$/+, n = 68) was significantly impaired compared to control flies (elav::GAL4/+, n = 45) $p = 0.002$.

Figure 4. *Drosophila* Oga regulates bouton number in larval neuro-muscular junction (NMJ). Type 1b muscle 4 synapses from wandering third instar larvae were double-stained with anti-discs large 1 (*Dlg*, magenta) and anti-synaptotagmin (*Syt*, green). (A) Representative NMJs are shown for genetic background control, Oga^{KO} and Oga^{D133N}. Scale bar 20 μm. (B) Quantification of the total number of boutons based on *Syt* staining indicates increased number of synaptic boutons present in Oga^{KO} ($p = 0.019$, n = 30). Similar trend was apparent in Oga^{D133N} ($p = 0.209$, n = 27) compared to Control (n = 24) larvae. (one-way ANOVA with Tukey post hoc test). Data presented as mean ± SD.

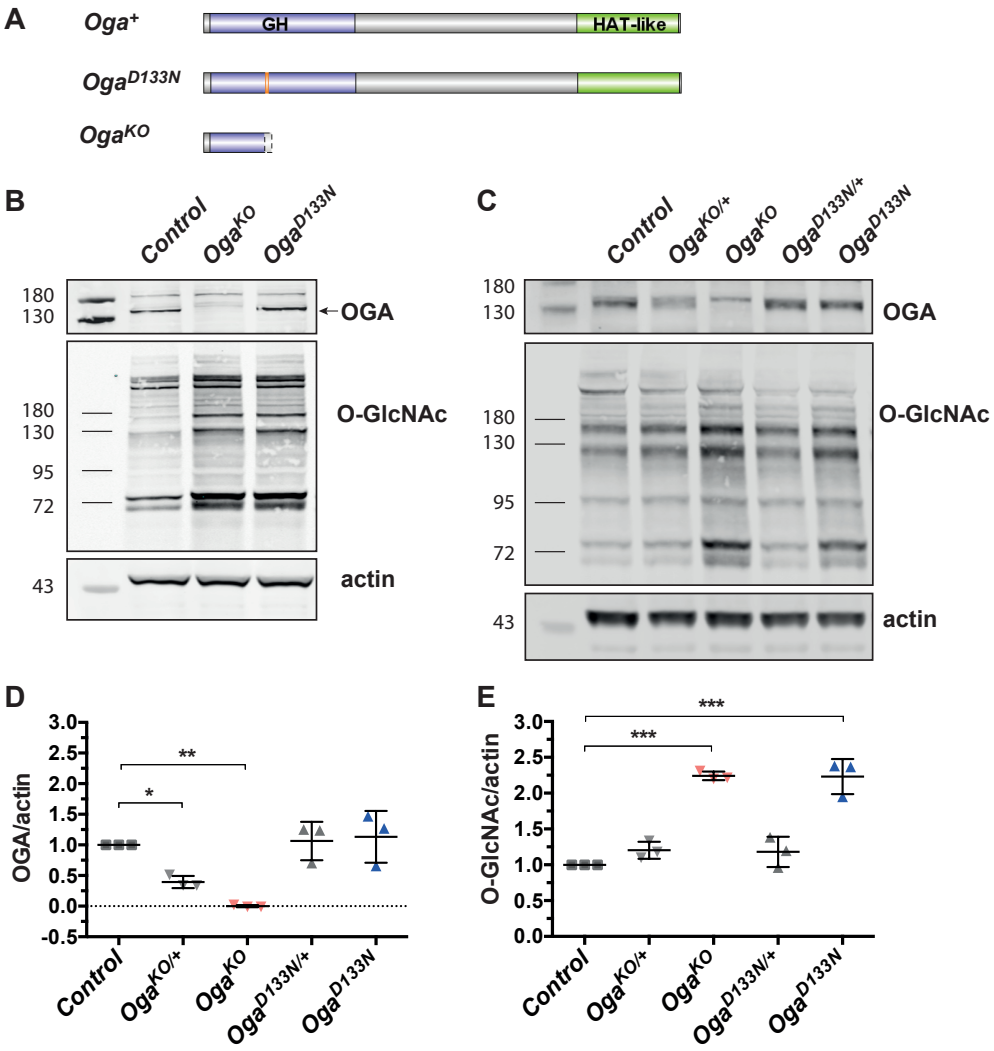

Figure 1. Generation and characterisation of *Oga^{D133N}* and *Oga^{KO}* alleles. (**A**) Schematic representation of *Drosophila melanogaster* Oga protein; purple glycosyl hydrolase (GH) domain, grey linker domain, green pseudo-histone acetyltransferase domain. The *Oga^{D133N}* allele expresses the full-length *Drosophila* Oga with a single D133N missense mutation in the GH domain (the mutation site is in orange). The *Oga^{KO}* allele only produces a short, truncated polypeptide of 148 amino acids terminating before the catalytic core of Oga GH domain. (**B**) Western blot on 4-8 h old *Drosophila* embryo samples indicate lack of Oga expression in OgaKO line and increased level of O-GlcNAcylation in homozygous *Oga^{KO}* and *Oga^{D133N} Drosophila* embryos. Embryos were collected from crosses of homozygous *Oga^{KO}* or *Oga^{D133N}* parental flies. Western blot was probed with an anti-OGA antibody and a monoclonal anti-O-GlcNAc antibody (RL2), raised against O-GlcNAc modified nucleoporins, that recognizes a subset of the O-GlcNAc modified proteome. Actin was used as a loading control. Complete loss of the lower band corresponding to Oga protein was apparent in homozygous (*Oga^{KO}*) samples. (**C**) Western blot on 1-4 days old male adult head lysates was probed with an anti-OGA antibody and monoclonal anti-O-GlcNAc antibody (RL2). Actin was used as a loading control. The anti-OGA antibody recognizes two proteins at the molecular weight range of 130-180 kDa, the lower band is specific to *Drosophila* Oga and the upper band is non-specific. Complete loss of the lower band was apparent in homozygous *Oga^{KO}* samples. (**D**) Quantification of Oga protein levels in adult head samples revealed that heterozygous *Oga$^{KO/+}$* flies have reduced Oga protein compared to genetic background control (one-way ANOVA with Dunnett's multiple comparisons test, $p = 0.036$, n = 3). Oga protein levels are unchanged in heterozygous *Oga$^{D133N/+}$* and homozygous *Oga^{D133N}* samples ($p = 0.9914$ and $p = 0.9013$, respectively). mean ± SD is shown. (**E**) Quantification of O-GlcNAcylated proteins revealed that *Oga^{KO}* and *Oga^{D133N}* flies have increased O-GlcNAc levels compared to genetic background control (2.2-fold, one-way ANOVA with Dunnett's multiple comparisons test, $p < 0.0001$, n = 3 for both lines, mean ± SD is shown) *Drosophila* adult head samples.

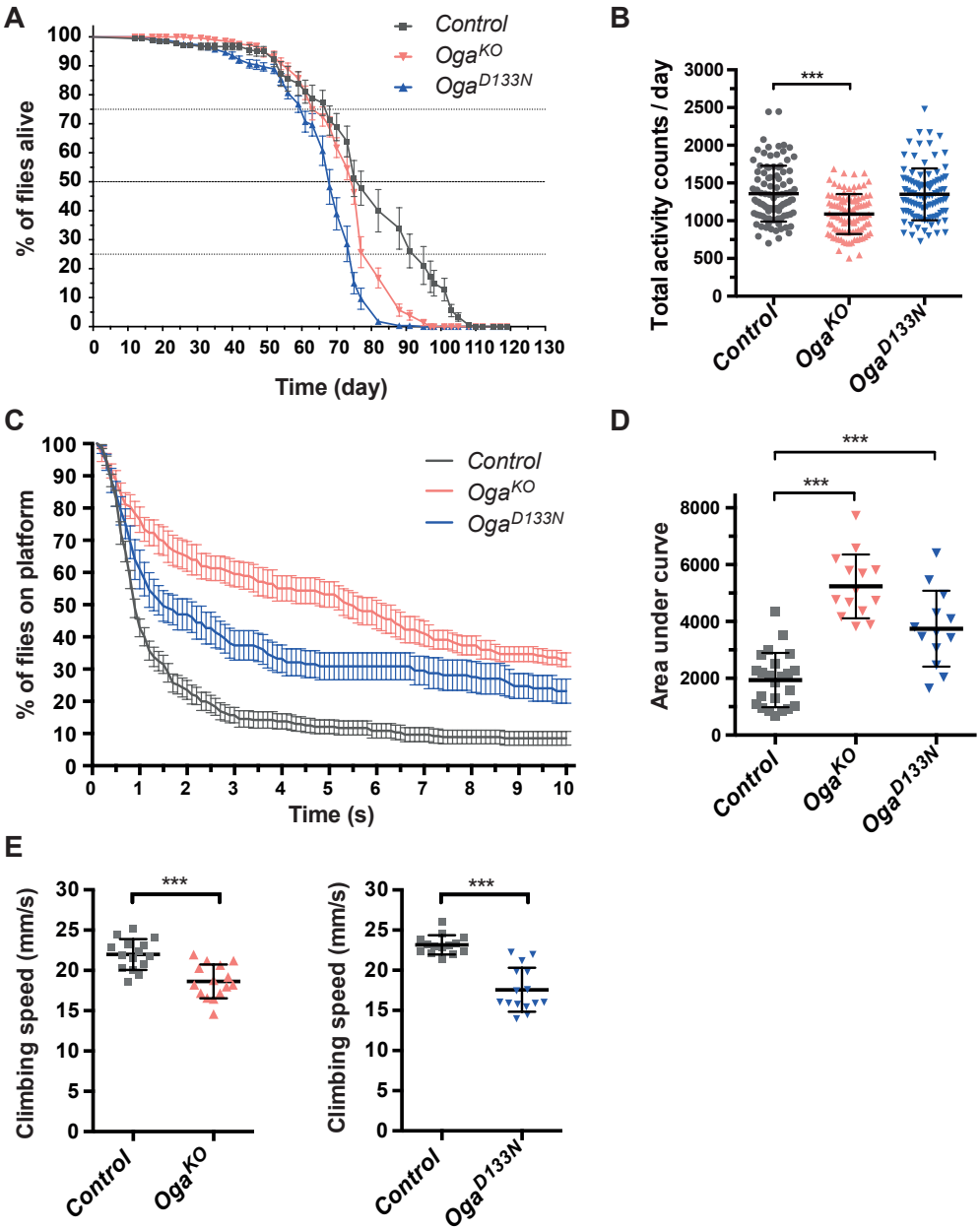

Figure 2. Lifespan and locomotor behaviour of *Oga*^{KO} and *Oga*^{D133N} flies. (**A**) Lifespan of homozygous *Oga*^{KO} and *Oga*^{D133N} male flies. Survival of 20 flies per vial was followed until no flies were left alive. Survivorship curves show mean ± SEM of data recorded from 9-14 vials/genotype, scoring the number of flies alive in every 2 days. Log-rank tests indicate decreased mean lifespan for *Oga*^{KO} (n = 280) and *Oga*^{D133N} (n = 280) flies compared to their genetic background control (n = 179) (Control vs *Oga*^{KO}, $\chi^2 = 41.5$, $p < 0.001$) (Control vs *Oga*^{D133N}, $\chi^2 = 104.8$, $p < 0.001$). (**B**) Total daily activity counts of control, *Oga*^{KO} and *Oga*^{D133N} male *Drosophila* plotted in 12:12 h light:dark cycle. *Oga*^{KO} (n = 101) exhibited decreased daily activity compared to control flies (n = 97) ($p < 0.001$, one-way ANOVA with Bonferroni's multiple comparisons test). (**C**) Locomotion and flight performance were assessed in the island assay. 15 flies per measurement were thrown on a white platform surrounded with water. Graphs show per cent of flies that remain on the platform over time (10 s). Mean ± SEM, for control n = 23, *Oga*^{KO} n = 13, *Oga*^{D133N} n = 14 repeats, data was collected over 3 days of measurement. (**D**) Floating bars depicting mean ± SD area under curve (AUC) based on the graphs shown in (D), one-way ANOVA with Holm-Sidak's multiple comparisons of mean AUC. Flight escape performance of *Oga*^{KO} and *Oga*^{D133N} flies was impaired compared to control (*Oga*^{KO} $p < 0.0001$; *Oga*^{D133N} $p = 0.0004$) (**E**) Climbing locomotor behaviour of Oga deficient flies was assessed based on their climbing speed (mm/s) in an automated negative geotaxis assay. *Oga*^{D133N} and *Oga*^{KO} groups showed significantly reduced climbing speed compared to background control indicating locomotor dysfunction. mean ± SD (Nonparametric Mann-Whitney test, Control n = 14, *Oga*^{D133N} n = 15, $p < 0.0001$; Control n = 15, *Oga*^{KO} n = 15, $p = 0.0002$).

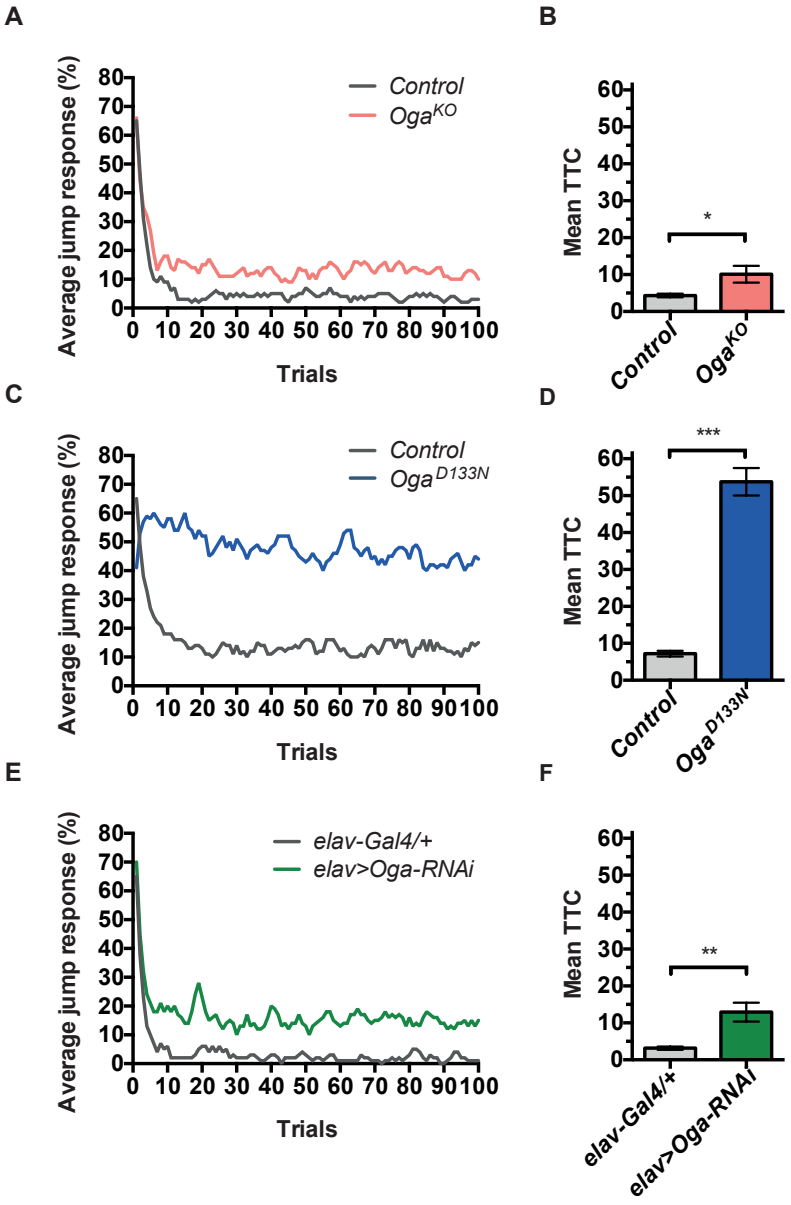

Figure 3. Loss of Oga activity in *Drosophila* affects non-associative learning in the light-off jump reflex habituation paradigm. Jump responses of 3–7-day-old individual male flies were induced by repeated light-off pulses (100 trials) with a 1 s inter-trial interval. Habituation was scored as the mean number of trials required to reach the no-jump criterion (TTC). Jump response curves show the average jump response (% of jumping flies) over 100 light-off trials at 1 s inter-trial interval. The number of trials needed to reach the no-jump criterion is presented as Mean TTC ± SEM. (**A**) and (**B**) Habituation of homozygous Oga^{KO} male flies (n = 63) was significantly slower compared to control flies (n = 65) p = 0.030. (**C**) and (**D**) Habituation of homozygous Oga^{D133N} male flies (n = 86) was significantly slower compared to control flies (n = 74) $p < 0.001$. (**E**) and (**F**) Habituation of adult flies with neuronal knock-down of *Oga*, (*elav::GAL4/+; UAS-OgaRNAi*$^{41822/+}$, n = 68) was significantly impaired compared to control flies (*elav::GAL4/+*, n = 45) p = 0.002.

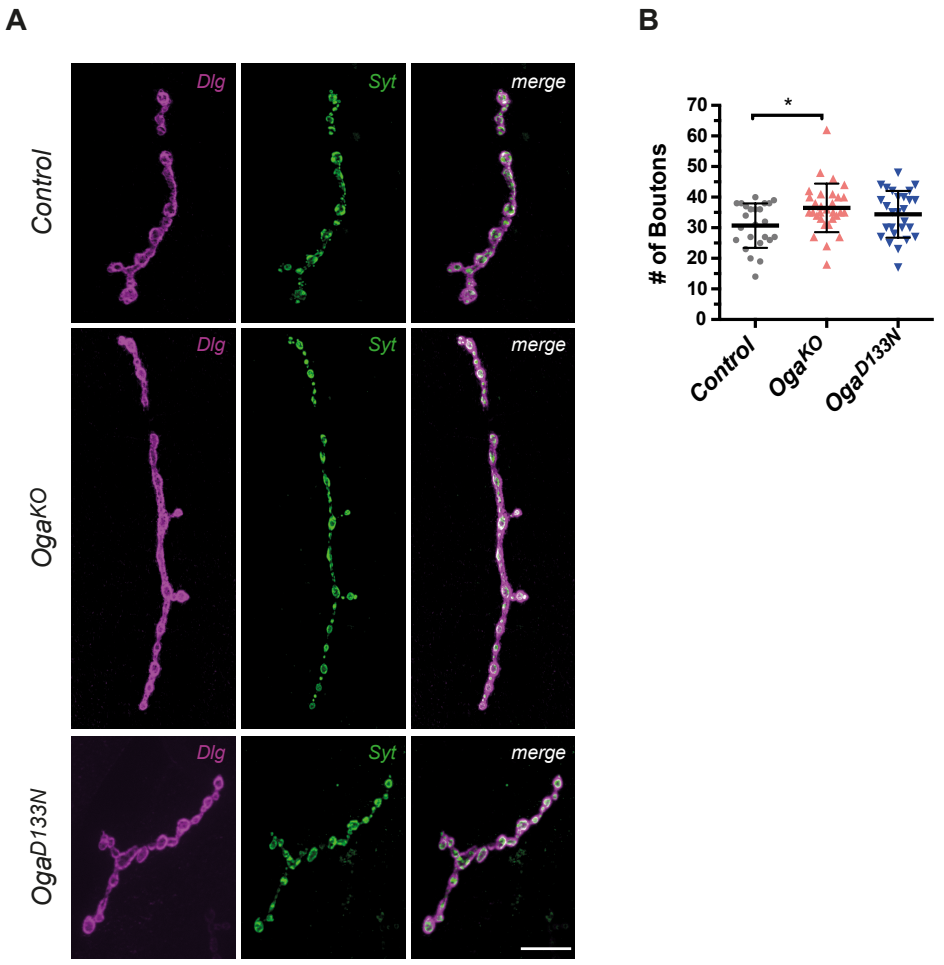

Figure 4. ***Drosophila*** **Oga regulates bouton number in larval neuro-muscular junction (NMJ).** Type 1b muscle 4 synapses from wandering third instar larvae were double-stained with anti-discs large 1 (*Dlg*, magenta) and anti-synaptotagmin (*Syt*, green). (**A**) Representative NMJs are shown for genetic background control, Oga^{KO} and Oga^{D133N}. Scale bar 20 µm. (**B**) Quantification of the total number of boutons based on *Syt* staining indicates increased number of synaptic boutons present in Oga^{KO} (p = 0.019, n = 30). Similar trend was apparent in Oga^{D133N} (p = 0.209, n = 27) compared to Control (n = 24) larvae. (one-way ANOVA with Tukey post hoc test). Data presented as mean ± SD.